Journal of
Mechanical
Science and
Technology

Journal of Mechanical Science and Technology 21 (2007) 1425~1434

Numerical Study of Fluid Force Reduction on a Circular Cylinder Using Tripping Rods

C. Y. Zhou*, L. Wang, W. Huang

Shenzhen Graduate School, Harbin Institute of Technology, Shenzhen 518055, China

(Manuscript Received December 20, 2006; Revised May 10, 2007; Accepted May 25, 2007)

Abstract

A numerical investigation on the effects of small tripping rods on the fluid force reduction on a big structure has been carried out using finite volume method where a configuration of a circular cylinder with two small tripping rods symmetrically placed very near to its front surface is studied. The diameter ratio of the rods and the cylinder is set at 0.08, 0.10 and 0.12, and the gap between the rods and the cylinder is fixed at 0.08 of the cylinder diameter. The angular position of the rods varies from 20° to 60°. The effects of the tripping rods on force reduction, vortex shedding frequency and flow separation have been examined for various arrangements of the rods with Reynolds number focused on 200 for laminar flow and $5.5x10^4$ for a turbulent flow. The results reveal that there exits an optimum position where the time averaged force coefficients acting on the cylinder all reach their minimum values and at the same time Strouhal number meets its maximum. At the optimum position the drag coefficient is reduced by 18% for Re=200 and 59% for Re=$5.5x10^4$. Further investigation with tripping rods placed near the separation points is also carried out for Re=$5.5x10^4$ and a considerable drag reduction is found.

Keywords: Circular cylinder; Tripping rod; Drag reduction

1. Introduction

Flow over a circular cylinder is practically related to many engineering applications, such as a vertical column of a tension leg platform or a riser pipe in waves or a current in the sea, road vehicles, buildings and bridges. The flow wake of the cylinder can generate unsteady forces which have the potential to damage the structural integrity of body. Research on this configuration often arises from the interest to understand the loads on the structure due to the fluid motion and further control the fluid flow to reduce the fluid force which may cause structural damages under certain unfavorable conditions. The ability to control a flow field actively or passively to obtain a desired change is of immense technological importance. In fact this has been hotly pursued by scientists and engineers. Many methods have been proposed over the recent years to control the wake vortex dynamics with the aim of suppressing the vortex shedding and reducing the drag force as well as the amplitude of the fluctuating lift. Typically, methods of control are to achieve transition delay, separation postponement, lift enhancement, drag reduction and turbulence augmentation. To achieve any of these end results, transition from laminar to turbulent flow may have to be either delayed or advanced, flow separation may have to be either prevented or provoked, and finally turbulent flow may have to be either suppressed or enhanced, such as the splitter plates and base bleed studied by Bearman (1965; 1967) which were used to suppress the vortex shedding, increase the formation

*Corresponding author. Tel.: +86 755 2596 1297, Fax.: +86 755 2603 3774
E-mail address: cyzhou@hit.edu.cn

length and reduce the base drag.

Using tripping rods to influence fluid force has been studied by many researchers. The mechanism of reducing drag by using tripping rods is that the tripping rods alter a subcritical flow into a transition flow or into a critical flow. A basic study was carried out by Fage and Warsap (1929). They placed two small tripping rods on the surface of a circular cylinder symmetrically at 65 degree angular position and investigated the effects of the rods on the drag force in the transition range of Re. They didn't study the effects of the angular position of the tripping rods on the drag force. James and Truong (1972) and Igarashi (1986) conducted experimental investigations on the effects of the various diameters and locations of tripping rods on the flow over a cylinder at Re=10^4–10^5 using tripping rods with d =0.6%D - 6.3%D. They found that the tripping rods with larger diameter caused the transition at an earlier Re and the optimum location of tripping rods for force reduction moved toward the stagnation point as the diameter of the tripping rod increases. With the tripping rods of d=0.6%D and 6.3%D the optimum angular position were found to be at 65° and 35° respectively. Nebres and Batill (1993) investigated the effects of large tripping rods on the characteristics of flow, steady drag and lift force, and Strouhal number using tripping rods with diameters of 0.7%D-14%D. The angular position of the tripping rods varied in the entire domain. They found that tripping rod had no effect on the flow characteristics when it was placed in the stagnation region or in the base region but it had a considerable effect when it was placed at an angular position of 20°-70°. The optimum position of the tripping rod for reducing fluid forces depends on the diameter of the tripping rod and the Reynolds number. For a low Reynolds number flow, Pearcey *et al.* (1982) pointed out that the diameters of the tripping rods must be quite large to modify the flow to a critical flow.

Investigations on the effects of the tripping rods on the fluctuating fluid forces have also been carried out. Hover *et al.* (2001) conducted a study on the effect of protrusions and attachments using thin wires attached on the surface of a smooth circular cylinder in a steady cross-stream. The impact of the wires on wake properties, and vortex-induced loads and vibration was examined at Reynolds numbers up to 4.6×10^4. They found that for a stationary cylinder, the tripping wires caused significant reductions in drag and lift coefficients, as well as an increase in the Strouhal number to a value around 0.25-0.27. For a forced oscillating cylinder, the main effects of the tripping wire were an earlier onset of frequency lock-in; changes in the phase of wake velocity and the dissipation of lift force. They also found that the flow-induced response of a flexibly mounted cylinder with attached wires is significantly altered as well, even far away from lock-in. Romberg and Popp (1998) investigated the effects of tripping rods on the flow-induced instability of a single flexibly mounted cylinder in a bundle. Recently, Alam *et al.* (2003) carried out an experimental investigation on effects of tripping rods on both steady and fluctuating fluid forces acting on a single circular cylinder and multiple cylinders. The Reynolds number was focused on 5.5×10^4. The optimum angular position of the tripping rod for force reduction was found to be 30 degree. Dramatic decreases were observed at this optimum angular position where the drag coefficient, fluctuating drag coefficient and fluctuating lift coefficient were reduced by 67%, 61% and 87%, respectively. Three different flow patterns were identified when the angular position was varied in the range of 20°-60°. The effect of a small control rod placed in the wake of a large cylinder was studied by Dalton *et al.* (2001) where the lift force suppression was examined using both CFD computation and flow visualization for Re up to 3000. A 2-D Large Eddy Simulation was used in the CFD study. They found that a noticeable influence on the drag and lift on the large cylinder was presented due to the placement of the small control rod in the wake. The suppression of lift was sensitive to the place where the rod was placed in the wake.

Not many numerical studies have been carried out to investigate the effects of tripping rod on flow characteristics. In this paper, with an aim to determine a detailed structure of the flow around a circular cylinder with two control tripping rods and the optimum position of tripping rods for fluid force reduction, a numerical work using finite volume method to simulate the fluid flow around a circular cylinder with two tripping rods symmetrically placed in front of it is conducted. The flow is assumed to be two dimensional and calculations for both laminar and turbulent flows are carried out. The Reynolds number is focused on 200 for laminar flow and 5.5×10^4 for turbulent flow. A further study on the effect of the tripping rods placed near the separation

points of the cylinder is also carried out and some primary results are presented.

2. Numerical method

2.1 Problem description

Figure 1 shows a schematic view of a circular cylinder with two tripping rods symmetrically placed near its front surface and the system is exposed in a coming uniform stream U_∞ where D is the diameter of the circular cylinder, d the diameter of the tripping rods, σ the spacing between the cylinder and the tripping rod, and α the position angle of the tripping rod. The coming uniform flow is assumed to be two dimensional and incompressible. A Cartesian coordinate system (x, y) is used to describe the flow where the x axis is aligned with the incoming flow direction and y axis is perpendicular to the stream direction.

2.2 The governing equation

The governing equations for the two dimensional incompressible fluid flow are the continuity equation and the Navier-Stokes equation:

$$\frac{\partial u_i}{\partial x_i} = 0 \tag{1}$$

$$\frac{\partial u_i}{\partial t} + u_j \frac{\partial u_i}{\partial x_j} = -\frac{1}{\rho}\frac{\partial p}{\partial x_i} + \frac{\partial}{\partial x_j}\left[\nu \frac{\partial u_i}{\partial x_j}\right] \tag{2}$$

where u_i is the velocity components, p is the pressure, ρ is the fluid density and ν is the kinematic viscosity. The calculation domain is a $50D \times 10D$ rectangular as illustrated in Fig. 2. At the inlet of the domain, a boundary condition of a constant velocity U_∞ is

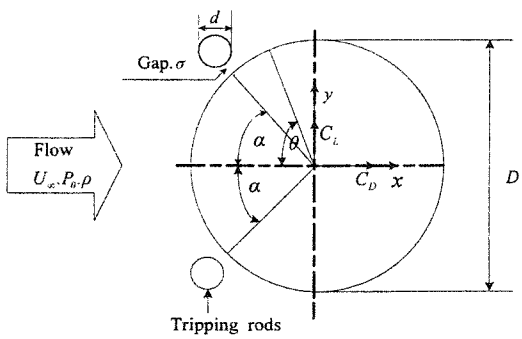

Fig. 1. Configuration of a circular cylinder with two tripping rods.

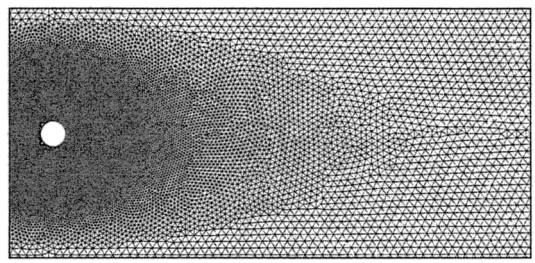

Fig. 2. Unstructured mesh in calculation domain.

specified, and at the outlet a Neumann type boundary condition $\frac{\partial u_i}{\partial n} = 0$ is assumed. On the surfaces of the cylinder and the tripping rods a no slip condition u_i=0 is applied.

2.3 Numerical method

The pressure-velocity based finite volume method is used on an unstructured mesh to solve the governing equations. The time derivative is discretized by a second-order backward implicit differencing scheme, and convective term by a second-order upwind differencing scheme and a second order central differencing scheme for the diffusive term. In solving the final resulting algebraic equation system the SIMPLER algorithm is applied. With this algorithm at each time step an intermediate velocity is calculated first and as the intermediate velocity generally does not satisfy the continuity equation, a correction is then calculated to update the velocity. This correction procedure is repeated in the time step until the mass flow residual for each mesh satisfies a given procession. Then the time marches into the next step.

2.4 Turbulence models

The Reynolds number is defined based on the diameter of cylinder as $Re = U_\infty D/\nu$ where $\nu = \nu_0 + \nu_t$ and ν_0 is the fluid kinematic viscosity and ν_t is the turbulence kinematic viscosity. Calculation for both laminar and turbulence flows are carried out. For laminar calculation the Reynolds number is kept at 200 and for turbulent calculation the Reynolds number is 5.5×10^4 where the RNG k-ε turbulence model is applied to the 2-D flow field. For turbulence flow the N-S Eq. (2) becomes the following Reynolds averaged N-S equation with new unknowns $\overline{u_i' u_j'}$

$$\frac{\partial u_i}{\partial t}+u_j\frac{\partial u_i}{\partial x_j}=-\frac{1}{\rho}\frac{\partial p}{\partial x_i}+\frac{\partial}{\partial x_j}\left[\nu\frac{\partial u_i}{\partial x_j}-\overline{u_i'u_j'}\right] \quad (3)$$

$$\overline{u_i'u_j'}=\frac{2}{3}k\delta_{ij}-\nu_t\left(\frac{\partial u_i}{\partial x_j}+\frac{\partial u_j}{\partial x_i}\right) \quad (4)$$

where $\rho\overline{u_i'u_j'}$ is the Reynolds stress and δ_{ij} the Kronecker Delta number. Equation (3) is solved coupled with the following equations for the turbulent kinetic energy k and the turbulence dissipation rate ε

$$\frac{\partial k}{\partial t}+u_j\frac{\partial k}{\partial x_j}=\frac{\partial}{\partial x_j}\left[a_k\nu\frac{\partial k}{\partial x_j}\right]+2\nu_t S_{ij}S_{ij}-\varepsilon \quad (5)$$

$$\frac{\partial \varepsilon}{\partial t}+u_j\frac{\partial \varepsilon}{\partial x_j}=\frac{\partial}{\partial x_j}\left[a_\varepsilon\nu\frac{\partial \varepsilon}{\partial x_j}\right]-R+2c_1\frac{\varepsilon}{k}\nu_t S_{ij}S_{ij}-c_2\frac{\varepsilon^2}{k} \quad (6)$$

where $a_k=a_\varepsilon=1.39$, $c_1=1.42$, $c_2=1.68$, $S_{ij}=\partial u_i/\partial x_j+\partial u_j/\partial x_i$ and $R=2\nu S_{ij}\dfrac{\overline{\partial u_i'}}{\partial x_j}\dfrac{\overline{\partial u_i'}}{\partial x_i}$

$$=\frac{c_\mu\eta^3(1-\eta/\eta_0)}{1+\beta\eta^3}\frac{\varepsilon^3}{k}$$

where $\eta=Sk/\varepsilon$, $S=(2S_{ij}S_{ij})^{1/2}$, $\eta_0=4.38$, $c_\mu=0.0845$ and $\beta=0.012$.

Near the wall of the cylinder and the tripping rods, further refined meshed is used so that calculation results with better procession may be obtained. The lift force F_y and drag force F_x subjected by the cylinder is obtained from the integrations of friction and pressure on the surface of the cylinder and the lift and drag coefficients C_L and C_D are defined by

$$C_L=\frac{2F_y}{\rho U_\infty^2 D} \text{ and } C_D=\frac{2F_x}{\rho U_\infty^2 D} \quad (7)$$

The averaged coefficients $\overline{C_L}$ and $\overline{C_D}$ are the time averaged values of C_L and C_D respectively, and the fluctuating coefficients C_{Lf} and C_{Df} are the r.m.s. values of C_L and C_D respectively.

2.5 Validation test

To validate the numerical method a calculation for a plain circular cylinder at Re=200 is carried out. The results for $\overline{C_D}$ and Strouhal number St are compared with previous published experimental and computational results in Table 1. Strouhal number St is defined as $St=fD/U_\infty$ where f is the vortex shedding frequency.

Table 1. $\overline{C_D}$ and St for a plain circular cylinder at Re=200.

Authors	St	$\overline{C_D}$
Present calculation	0.1893	1.3363
Braza[12] *et al.* (1986)	0.200	1.35
Giannakidis (1997)	0.190	1.25
Saltara[13] (1999)	0.190	1.25
Borthwick[14] (1986)	0.188	1.02
Roshko[15] (1954)(exp.)	0.17-0.19	
Norberg (1993)(exp.)		1.30

The comparison shows that the present results for $\overline{C_D}$ and St is in good agreement with previous published results.

3. Results and discussions

Calculations are carried out for both laminar and turbulence flows. For the laminar flow Re=200 and for turbulent flow $Re=5.5\times10^4$. The effects of the tripping rods with different angle position and different diameter on fluid forces, flow characteristics and Strouhal number are studied. Three diameter ratios d/D =0.08, 0.10 and 0.12 and four angle positions α=20°, 30°, 40°, 50° and 60° are considered. The gap spacing σ between the cylinder and the tripping rods is kept at $0.008D$ for all calculations.

3.1 Effects of tripping rods on fluid forces

The effects of tripping rod angular position α on force coefficients C_D, C_{Df} and C_{Lf} are shown in Figs. 3 and 4 for Re=200 and $Re=5.5\times10^4$, respectively. It can be seen from Fig. 3 that with the tripping rods the values of C_D, C_{Df} and C_{Lf} are generally reduced compared with those values for a plain cylinder when α≤50°, and increased when α>50°. The variations of C_D, C_{Df} and C_{Lf} with α have the same tendency. As α increases C_D, C_{Df} and C_{Lf} decrease first and reach their minimum values and then increase. There exists an optimum angular position for force reduction and it is found that for Re=200 this optimum position is α=40°. In the case of tripping rods with d/D =0.10, at this optimum position the drag force coefficient can be reduced by 18% [see Fig. 3(a)] which is much smaller than that for a flow with $Re=5.5\times10^4$ Alam *et*

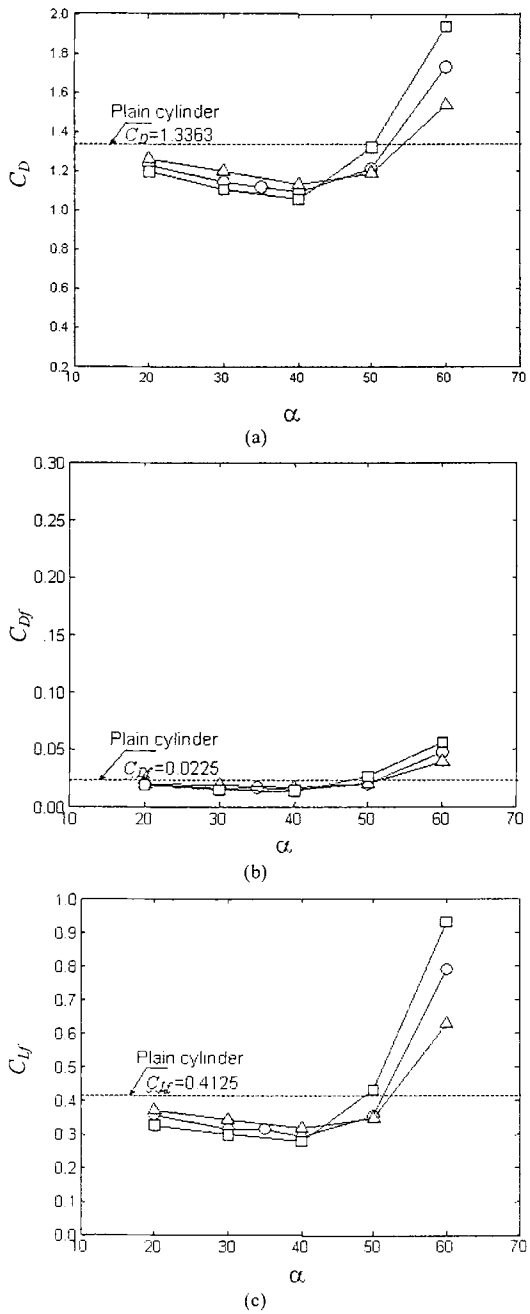

Fig. 3. Variations of force coefficients with the angle position of tripping rods, (a) C_D; (b) C_{Df}; (c) C_{Lf}; △, d/D=0.08; ○, d/D=0.10; □, d/D=0.12.

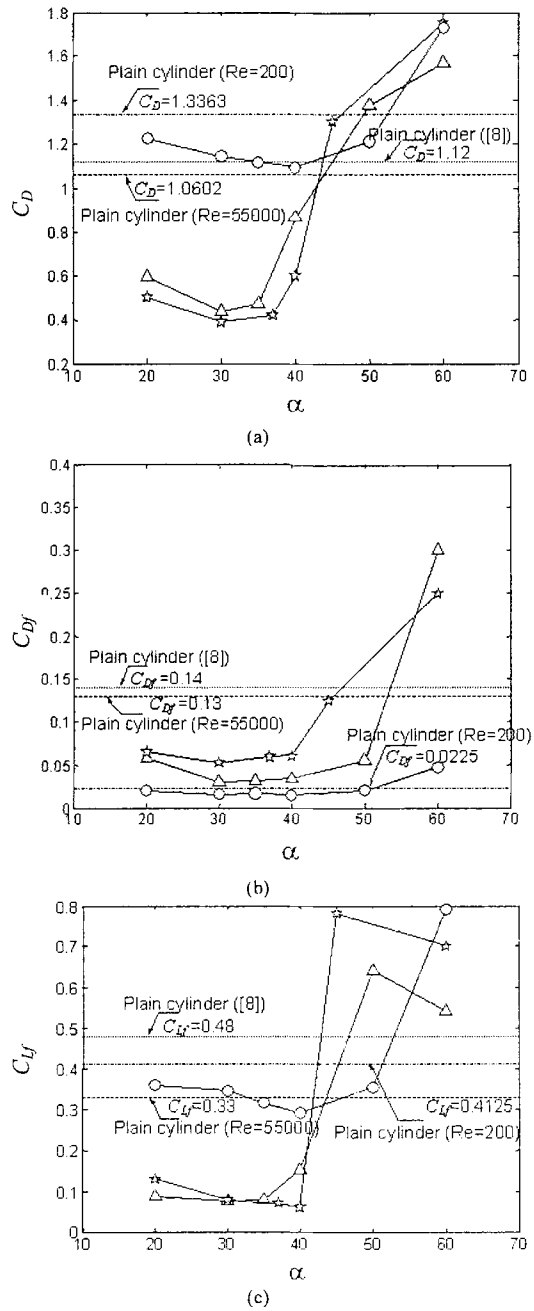

Fig. 4. Variations of force coefficients with α, (a) C_D; (b) C_{Df}; (c) C_{Lf}; Δ, Re=5.5×10^4; ○, Re=200; ☆, Re=5.5×10^4 [Alam *et al.* (2003)].

al. (2003). It is noted that the effect of d/D on the force coefficients is small when α≤50°, and becomes evident when α>50° where obviously tripping rods with larger value of d/D give more influence on the force coefficients.

In Fig. 4 the calculation results for d/D =0.10 at Re=5.5×10^4 are compared with the experimental data of [8]. Results for Re=200 are also included in the figure for comparison. The results show that the force coefficients are considerably reduced by using the

tripping rods with the angular position smaller than 40°. The optimum position for force reduction is α=30° at this Reynolds number and the drag coefficient C_D is reduced by 59%, C_{Df} by 78% and C_{lf} by 80% compared with that for a plain cylinder. The force coefficients for α=60° are much larger than those for a plain cylinder at the same Reynolds number. These results are similar to the experimental results of Alam *et al.* (2003). The present results of C_D generally agree with the experimental results by Alam *et al.* (2003) in the tendency of variation with α but slightly higher for α<45° and lower for α>45°. The comparison between the results for Re=200 and Re=5.5×10^4 indicates that as the Reynolds number increases, the optimum position for force reduction moves upward to the stagnation point. The result shows that the tripping rod has a better control effect for force reduction at higher Re.

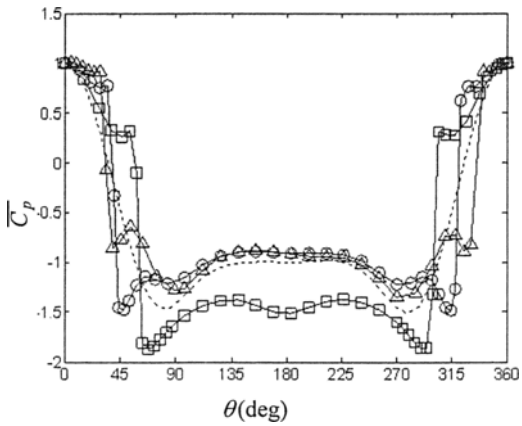

(a) Re=200; Δ, α=30°; O, α=40°; □, α=60°; ..., plain cylinder.

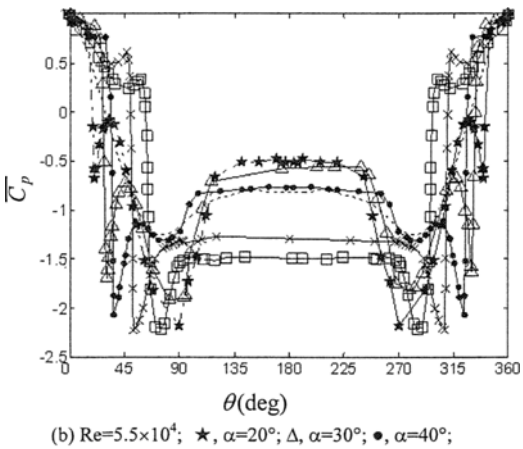

(b) Re=5.5×10^4; ★, α=20°; Δ, α=30°; •, α=40°; ×, α=50°; □, α=60°; ..., plain cylinder.

Fig. 5. Variation of surface pressure coefficient of main cylinder with α.

To see how the drag force is reduced the distributions of the time averaged pressure coefficient $\overline{C_p}$ on the cylinder surface for different values of α are plotted in Fig. 5 for Re=200 and Re=5.5×10^4, where C_p is defined as

$$C_p = 2\times(p - p_\infty)/\rho u_\infty^2 \tag{8}$$

and $\overline{C_p}$ is the time averaged value of C_p. For comparison the result of $\overline{C_p}$ for a plain cylinder is also given in the figure. Figure 5(a) shows that the magnitude of $\overline{C_p}$ for α=30° and 40° is little bit smaller than that for a plain cylinder in the range from 90° to 270°, and for α=60° the magnitude of $\overline{C_p}$ is much larger than that for the plain cylinder. The changes in C_p caused by the placement of tripping rods result in the variations in the drag coefficient. At higher Reynolds number Re=5.5×10^4 [see Figure 5(b)] the magnitude of $\overline{C_p}$ appears to be much smaller than that for a plain cylinder at the same Re on the back surface of the cylinder which results in a

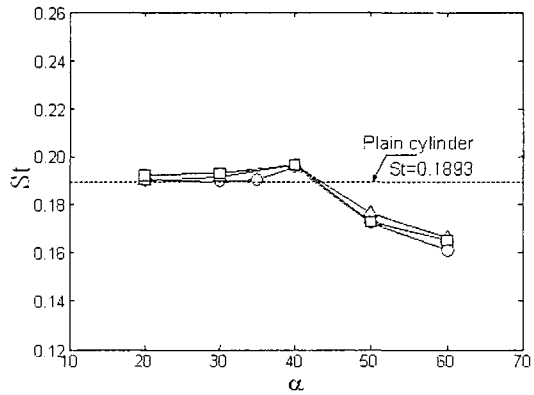

Re=200, Δ, *d*/*D*=0.08; O, *d*/*D*=0.10; □, *d*/*D*=0.12.

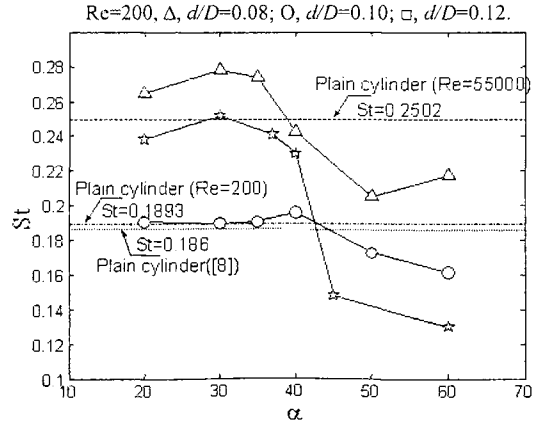

Re=5.5×10^4, Δ, *d*/*D*=0.08; O, *d*/*D*=0.10; □, *d*/*D*=0.12.

Fig. 6. Variation of Strouhal number with α.

considerable reduction in drag force. It is obvious that the effect of tripping rod for drag reduction is more effective at this Reynolds range.

3.2 Strouhal Number

At the same time when the force coefficients reach the minimum values, the Strouhal number is seen to obtain a maximum value. The influence of angular position of the tripping rods on the Strouhal number is illustrated in Fig. 6. As can be seen the variation trend of the Strouhal number with α is opposite to those of force coefficients. There is a quick decrease in St for α=35°-50°. This was found by Alam *et al.* (2003) and Nebre and Batill (1993). It was observed that two types of flow patterns appear intermittently in this range of α (Alam *et al.*, 2003).

3.3 The flow patterns and separation point

Figure 7 shows the comparison of the vorticity patterns around the cylinder between the plain cylinder and cylinder with tripping rods at α=40°.

It is seen from the figure that the flow pattern is very sensitive to the tripping rod at this position angle. It is observed that the vortex formation length becomes longer and the transverse spacing between the vortices turns to be smaller when there are the tripping rods placed in the front of the cylinder at α=40°. This indicates that the vortex shedding frequency increases.

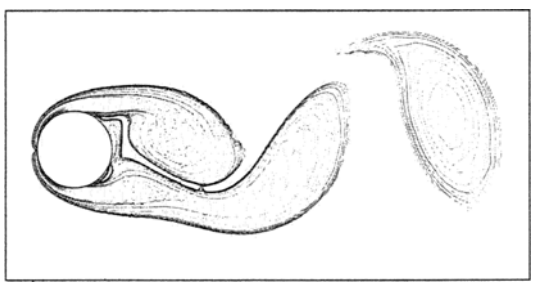

(a) Single cylinder

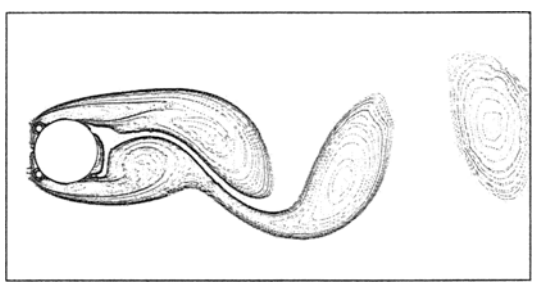

(b) Cylinder with tripping rods α=40°.

Fig. 7. Vorticity contours around the circular cylinder at Re=200.

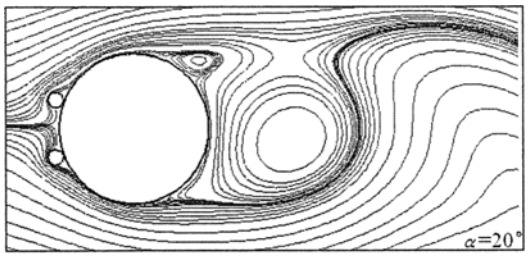

(a)

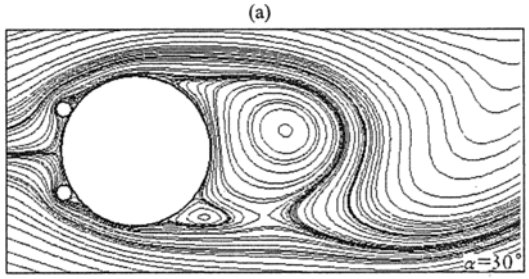

(b)

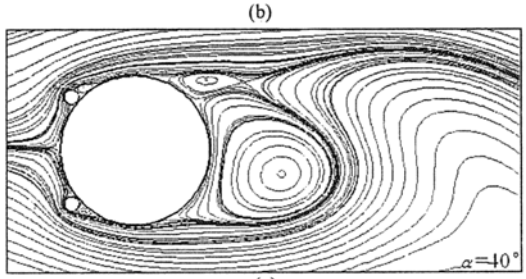

(c)

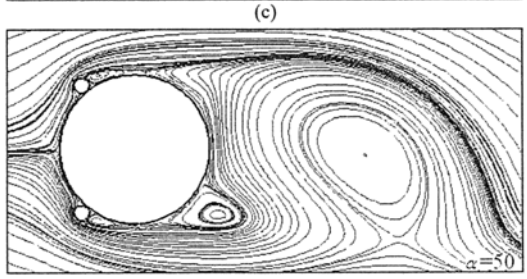

(d)

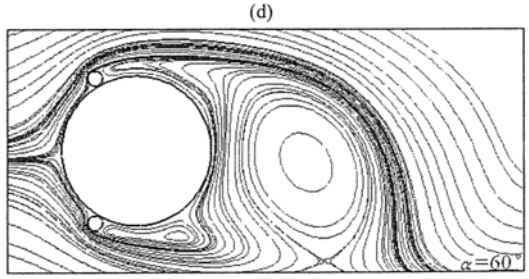

(e)

Fig. 8. Streamline around the cylinder for different position angle, Re=200.

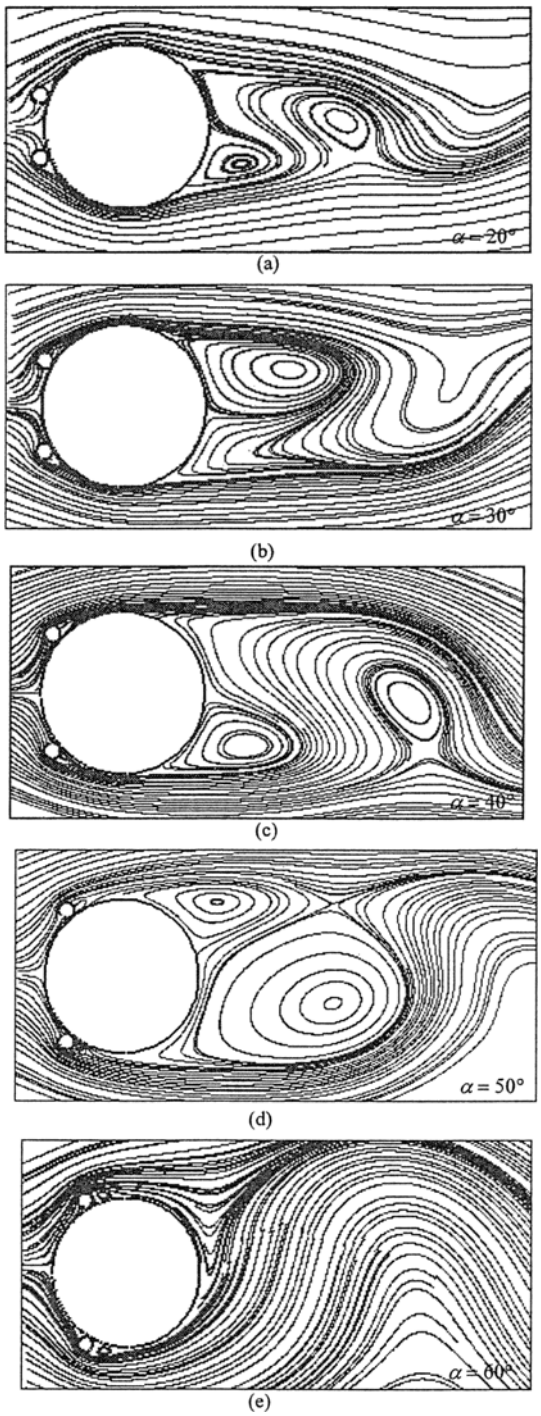

Fig. 9. Streamline around the cylinder for different angular position, Re=5.5×10^4.

Two groups of streamline patterns with different angle positions for Re=200 and Re=5.5×10^4 are illustrated in Figs. 8 and 9 respectively. It is obvious to see that as the tripping rods placing angle α varies the separation point changes. The position of the separation point can be determined by considering $\partial v_s / \partial r|_{r=0}=0$ on the surface where v_s is the tangential velocity. The results for different angular positions are listed in Table 2 for both Re=200 and Re=5.5×10^4.

Table 2. The variation of separation point position with α.

α	20°	30°	40°	50°	60°
Re=200	112°	116°	112°	50°	67°
Re=5.5×10^4	128°	131°	122°	68°	51°

When α=20°, the fluid flow attaches on the surface of the cylinder immediately after flowing over the tripping rods. Flow separates from the surface of the cylinder at an angle of 112°. When α=30°, the flow does not attach on the surface of cylinder immediately after separates from the tripping rods but generates a small vortex at the corner formed between the cylinder and the tripping rods. The flow reattaches on the surface of the cylinder and separates at an angle of 116°. This is more obvious when α=40°. When the position angle increases up to 50° and 60°, the flow separates from the tripping rods and not reattach on the cylinder any more. This forms a much large recirculation region.

The recirculation regions for α=50° and α=60° are wider than that for α<40°. This is corresponds to a relatively large reverse force and subsequent a larger drag force. At high Re, the separation points moves downwards for α=20°, 30° and 40°, while for α=50°, 60° the separation point moves upwards.

3.4 Further investigations with tripping rods around separation points

Further investigations with tripping rods near the separation points for Re=5.5×10^4 are carried out where *d/D* is kept at 0.10, the gap spacing σ is fixed at 0.006*D* and position angle α takes the values 120°, 130°, 139°, 145° and 150°. A group of primary results of this study is shown in Figs. 10-12. It is found that tripping rods have a considerable effect on the flow characteristics and more fluid force reduction can be achieved compared to the situation when tripping rods are placed near the front surface of the cylinder. Figure 10 shows the variation of force coefficients C_D with the position angle α. It is seen that when α=139°,

the drag coefficient C_D reaches a minimum value of 0.286 which indicates a tremendous drag reduction by as high as 73% compared to that for a plain cylinder at the same Re. It is worthy to notice that $\alpha = 139°$ is the separation point of a plain cylinder at Re=5.5×10^4 in the present calculation. The drag coefficient increases sharply with the angle position of the rods after the separation point and the effect of the rod becomes less as the tripping rods move forwards into the base region of the cylinder.

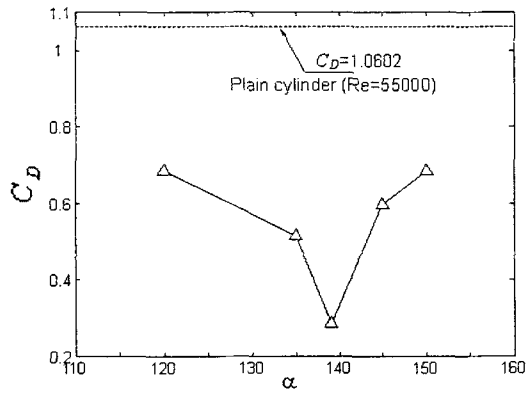

Fig. 10. Variation of drag coefficient C_D with α.

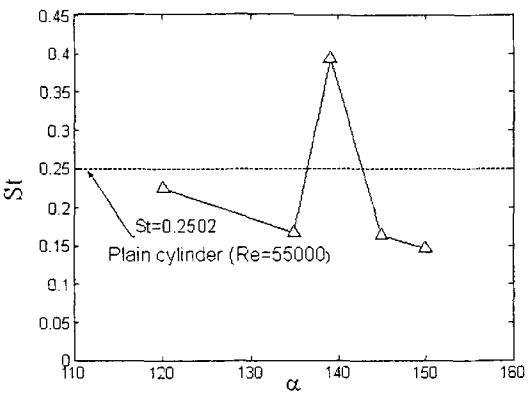

Fig. 11. Variation of Strouhal number with α.

The variation of the Strouhal number with the position angle is shown in Fig. 11. An opposite behavior around the separation point is observed as expected. The sharp reduction in C_D and increase St is closely related to the changes in flow characteristics. It is shown in Fig. 12 that the tripping rods for α=139° are just located at the shear layer, which smear and diffuse the very concentrated vorticity in the shear layers of early stage. The base pressure is affected by the altered shear layer in such a way that the pressure is decreased significantly and with virtually no oscillation as C_{DF} and C_{LF} are found to be near zero.

4. Conclusion

Investigation of tripping rods on force reduction is carried out in this paper using finite volume method, where a configuration of two tripping rods are symmetrically placed in front of a circular cylinder is studied. Calculations are conducted for both laminar

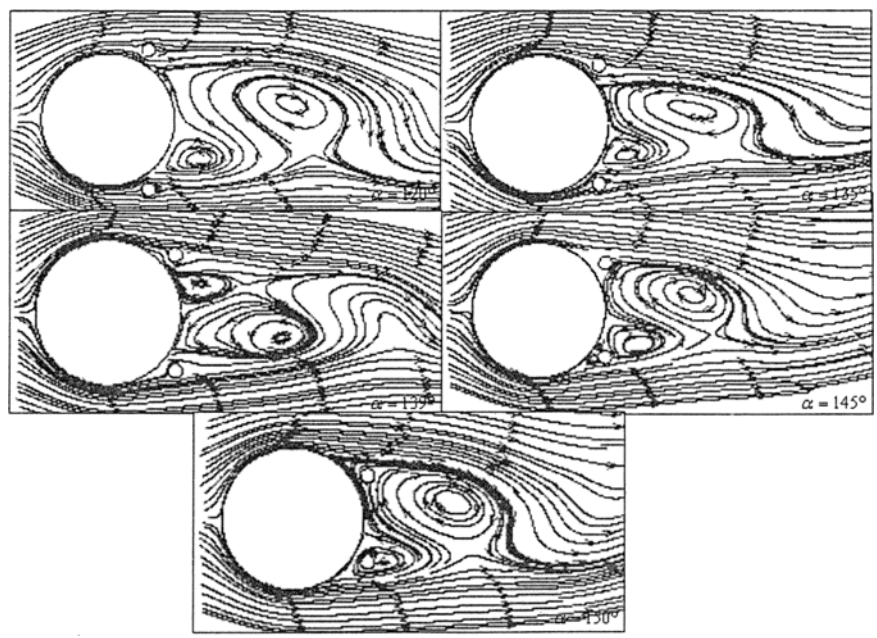

Fig. 12. Streamline around the cylinder for different position angle, Re=5.5×10^4.

and turbulence flows, and the Reynolds number is focused on 200 for laminar flow and 5.5×10^4 for turbulent flow. The effects of the angular position of the tripping rods, diameter ratio of the rod to cylinder and Reynolds number on force coefficients and Strouhal number and flow patterns are examined. It is found that the force subjected by the cylinder is very sensitive to the angular position of the tripping rods in the range of 30°-60°. There exists an optimum position where the force coefficient reaches its minimum and Strouhal number maximum. This optimum angular position for Re=200 is at α=40° where the drag coefficient is reduced by 18%, while for $Re=5.5\times10^4$ the optimum position is α=30° and the drag coefficient is reduced by 59% which is in good agreement with previous experimental data. Further numerical investigation on the effects of two tripping rods placed near the separation points are also studied and the primary results of this study show that the drag coefficient reduction can reach as high as 73%, and the drag and lift fluctuating force coefficients are near zero when the rods are placed at a selected location near the separation points.

References

Alam, M. M., Sakamoto, H. and Moriya, M., 2003, "Reduction of Fluid Forces Acting on a Single Circular Cylinder and two Circular Cylinders by using Tripping rods," *Journal of Fluids and Structures*, Vol. 18, pp. 347~366.

Bearman, P. W., 1965. "Investigation of flow Behind a Two-Dimensional Model with Blunt Trailing Edge and Fitted with Splitter Plates," *Journal of Fluid Mechanics*, Vol. 21, pp. 241~255.

Bearman, P. W., 1967, "The Effect of Base Bleed on the flow Behind a Two-Dimensional Model with a Blunt Trailing Edge," *The Aeronautical Quarterly*, Vol. 18, pp. 207~224.

Borthwick, A., 1986, "Comparison Between two Finite-Difference Schemes for Computing the flow Around a Cylinder." *International Journal for Numerical Methods in Fluids*, Vol. 6, p. 275.

Braza, M., Chassaing, P. and Minh, H. H. 1986, "Numerical Study and Physical Analysis of the Pressure and Velocity Fields in the Near Wake of a Circular Cylinder," *Journal of Fluid Mechanics*, Vol. 165, pp. 79~130.

Dalton, C., Xu, Y. and Owen, J. C., 2001, "The Suppression of Lift on a Circular Cylinder Due to Vortex Shedding at Moderate Reynolds Numbers," *Journal of Fluids and Structures*, Vol. 15, pp. 617~628.

Fage, A. and Warsap, J. H., 1929, "The Effects of Turbulence and Surface Roughness on the Drag of a Circular Cylinder," Aeronautical Research Council, Reports and Memoranda No. 1283, pp. 1~14.

Hover, F. S., Tvedt, H. and Triantafyllou, M. S., 2001, "Vortex-Induced Vibrations of a Cylinder with Tripping Wires," *Journal of Fluid Mechanics*, Vol. 448, pp. 175 ~195.

Igarashi, T., 1986, "Effect of Tripping Wires on the flow Around a Circular Cylinder Normal to an Airstream," *Bulletin of the Japan Society of Mechanical Engineers*, Vol. 29, pp. 2917~2924.

James, D. F. and Truong, Q. T., 1972, "Wind Load on a Cylinder with a Spanwise Protrusion," *Journal of the Engineering Mechanics Division, Proceedings of the American Society of Civil Engineers*, Vol. 98, pp. 1573 ~1589.

Nebres, J. and Batill, S., 1993, "Flow about a Circular Cylinder with a Single Large-Scale Surface Perturbation," *Experiments in Fluids*, Vol. 15, pp. 369~379.

Pearcy, H. H., Cash, R. F. and Salter, I. J., 1982, "Flow Past Circular Cylinders: Simulation of Full-Scale flows at Model Scale." National Maritime Institute, NMI Report, Vol. 131, pp. 1~54.

Romberg, O. and Popp, K., 1998, "The Influence of Trip-wires on the Fluid-Damping-Controlled Instability of a Flexible Tube in a Bundle," *Journal of Fluids and Structures*, Vol. 12, pp. 17~32.

Roshko, A., 1954, "On the Drag and Shedding Frequency of two Dimensional Bluff Bodies," Technical Note 3169, National Advisory Committee for Aeronautics (NACA), Washington.

Saltara, F., 1999, "Numerical Simulation of the flow about Circular Cylinders," Ph. D. thesis, EPUSP University of São Paulo, Brazil.